

TRIM25 RING-finger E3 ubiquitin ligase is essential for RIG-I-mediated antiviral activity

Michaela U. Gack^{1,2}, Young C. Shin¹, Chul-Hyun Joo^{1,3}, Tomohiko Urano^{4,5}, Chengyu Liang¹, Lijun Sun⁶, Takeuchi Osamu⁷, Shizuo Akira⁷, Zhijian Chen⁶, Satoshi Inoue^{4,5} & Jae U. Jung¹

Retinoic-acid-inducible gene-I (RIG-I; also called DDX58) is a cytosolic viral RNA receptor that interacts with MAVS (also called VISA, IPS-1 or Cardif) to induce type I interferon-mediated host protective innate immunity against viral infection^{1–6}. Furthermore, members of the tripartite motif (TRIM) protein family, which contain a cluster of a RING-finger domain, a B box/coiled-coil domain and a SPRY domain, are involved in various cellular processes, including cell proliferation and antiviral activity⁷. Here we report that the amino-terminal caspase recruitment domains (CARDs) of RIG-I undergo robust ubiquitination induced by TRIM25 in mammalian cells. The carboxy-terminal SPRY domain of TRIM25 interacts with the N-terminal CARDs of RIG-I; this interaction effectively delivers the Lys 63-linked ubiquitin moiety to the N-terminal CARDs of RIG-I, resulting in a marked increase in RIG-I downstream signalling activity. The Lys 172 residue of RIG-I is critical for efficient TRIM25-mediated ubiquitination and for MAVS binding, as well as the ability of RIG-I to induce antiviral signal transduction. Furthermore, gene targeting demonstrates that TRIM25 is essential not only for RIG-I ubiquitination but also for RIG-I-mediated interferon- β production and antiviral activity in response to RNA virus infection. Thus, we demonstrate that TRIM25 E3 ubiquitin ligase induces the Lys 63-linked ubiquitination of RIG-I, which is crucial for the cytosolic RIG-I signalling pathway to elicit host antiviral innate immunity.

A recent series of studies has identified RIG-I and melanoma differentiation-associated gene 5 (MDA5; also called IFIH1) as cytosolic receptors for viral double-stranded RNA and 5' triphosphate RNA^{2,4,6}. RIG-I and MDA5 belong to the DExD/H box RNA helicase family, the members of which contain two caspase recruitment domains (2CARD) in the N-terminal region and a potential ATP-dependent RNA helicase activity in the C-terminal region^{8,9}. To decipher the cytosolic RIG-I-mediated antiviral signalling pathway, we attempted to identify cellular proteins associated with the N-terminal 2CARD of RIG-I and MDA5 using mammalian glutathione *S*-transferase (GST) fusion constructs. Polypeptides with apparent molecular masses of 52, 60 and 68 kDa were present specifically in the GST–RIG-I(2CARD) complex but not in the GST–MDA5(2CARD) complex or with GST alone (Fig. 1a). Notably, mass spectrometry and immunoblotting showed that these polypeptides were exclusively identified as ubiquitinated forms of GST–RIG-I(2CARD) (Supplementary Fig. 1a). To confirm RIG-I ubiquitination, HEK293T cells were co-transfected with Flag-tagged full-length RIG-I or a RIG-I mutant in which the 2CARD had been deleted (RIG-I(Δ 2CARD)) together with haemagglutinin (HA)-tagged ubiquitin.

RIG-I, but not RIG-I(Δ 2CARD), was extensively ubiquitinated (Fig. 1b and Supplementary Fig. 1b). In addition, anti-HA immunoblotting detected ubiquitinated Flag-tagged RIG-I as multiple species with apparent molecular masses of 120–150 kDa, significantly larger than unmodified Flag–RIG-I (Fig. 1c, top left panel). Furthermore, Sendai virus infection and/or interferon (IFN)- β treatment resulted in the markedly increased ubiquitination of endogenously or exogenously expressed RIG-I (Fig. 1c and Supplementary Fig. 1c). These results indicate that RIG-I undergoes robust ubiquitination at its N-terminal 2CARD and that this ubiquitination apparently increases on viral infection.

To dissect further the ubiquitination of the 2CARD of RIG-I, which contains 18 lysine residues, the *in vivo* ubiquitinated forms of N-terminal GST-fused and C-terminal Flag-tagged RIG-I(2CARD) were purified and analysed by multi-dimensional liquid chromatography coupled with tandem mass spectrometry (LC/LC-MS/MS; Fig. 1a, d, bands 1–3). Both GST–RIG-I(2CARD) and Flag–RIG-I(2CARD) carried the ubiquitin peptides at Lys 99, 169, 172, 181, 190 or 193 (Fig. 1d). Additional mass spectrometry analysis showed that band 2 and 3 fragments carried the unique, branched Gly–Gly signature peptides primarily with the ubiquitin Lys 63 linkage (Fig. 1d). Furthermore, GST–RIG-I(2CARD) and full-length RIG-I were strongly ubiquitinated when HA-tagged wild-type ubiquitin or a K48R ubiquitin mutant was expressed, whereas their ubiquitination was significantly reduced upon expression of a K63R ubiquitin mutant protein (Supplementary Fig. 2). These results indicate that the second CARD of RIG-I is the primary site for Lys 63-linked ubiquitination.

To corroborate the ubiquitination of the 2CARD of RIG-I, six lysine residues were replaced with arginine (K \rightarrow R) individually and in various combinations; these mutants were then tested for their ubiquitination level. The K172R mutation (alone or together with other mutations) caused near-complete loss of ubiquitination of the 2CARD of RIG-I (Fig. 1e and Supplementary Fig. 3a). In contrast, other K \rightarrow R mutations had little or no effect on ubiquitination of the RIG-I 2CARD (Fig. 1e). As previously shown¹⁰, wild-type GST–RIG-I(2CARD) potentially induced IFN- β and NF- κ B promoter activity (Fig. 1f and Supplementary Fig. 3b). GST–RIG-I(2CARD) mutants containing the K172R mutation alone or together with other mutations showed markedly reduced IFN- β and NF- κ B promoter activation, consistent with their lack of ubiquitination; in contrast, other GST–RIG-I(2CARD) mutants induced IFN- β and NF- κ B promoter activity as strongly as wild-type GST–RIG-I(2CARD) (Fig. 1f and Supplementary Fig. 3b). These results suggest that Lys 172 is the essential site for RIG-I 2CARD ubiquitination and signalling activity

¹Department of Microbiology and Molecular Genetics and Tumor Virology Division, New England Primate Research Center, Harvard Medical School, 1 Pine Hill Drive, Southborough, Massachusetts 01772, USA. ²Institute for Clinical and Molecular Virology, Friedrich-Alexander University Erlangen-Nuremberg, 91054 Erlangen, Germany. ³Department of Microbiology, University of Ulsan College of Medicine, Seoul 138-736, South Korea. ⁴Department of Geriatric Medicine, Graduate School of Medicine, The University of Tokyo, 7-3-1 Hongo, Bunkyo, Tokyo 113-8655, Japan. ⁵Research Center for Genomic Medicine, Saitama Medical School, Saitama 350-124-2, Japan. ⁶Department of Molecular Biology, University of Texas Southwestern Medical Center, Dallas, Texas 75390-9148, USA. ⁷Department of Host Defense, Japan Science and Technology Agency, Osaka 565-0871, Japan.

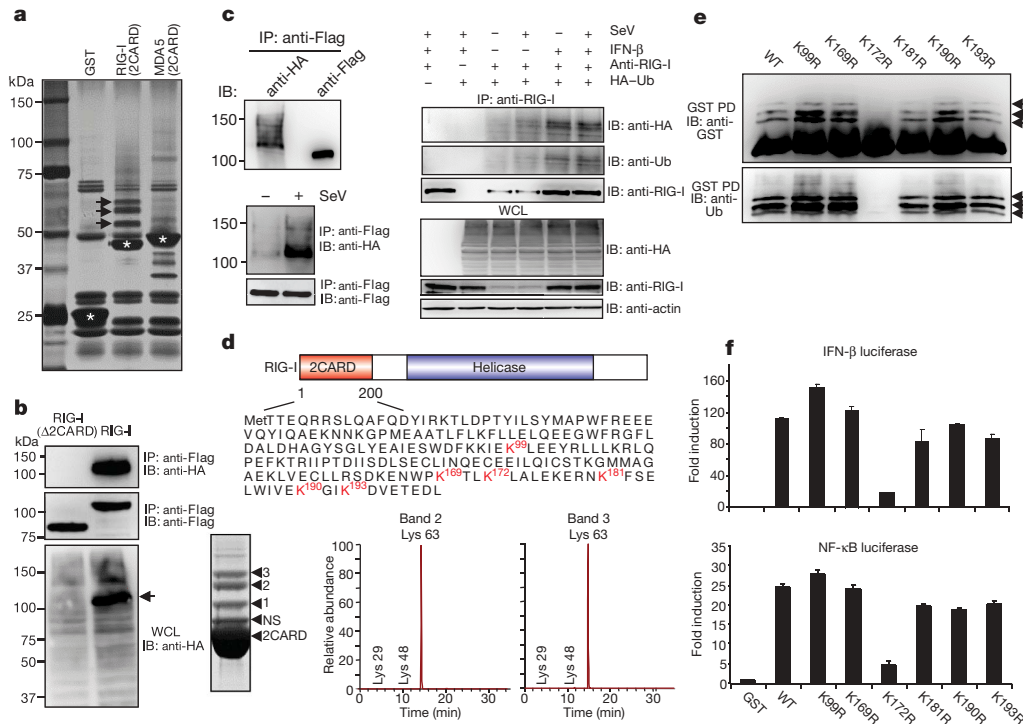


Figure 1 | The 2CARD of RIG-I undergoes robust ubiquitination. **a**, Silver-stained purified GST fusion complexes. Arrows, unique bands; asterisks, GST fusions. **b**, **c**, HEK293T cells transfected with Flag-RIG-I (**b**, and **c**, top-left) or Flag-RIG-I(Δ 2CARD) (**b**) together with HA-ubiquitin were used for immunoprecipitation (IP) and immunoblotting (IB). WCL, whole cell lysate. **c**, Bottom-left panel: HEK293T cells transfected with Flag-RIG-I and HA-ubiquitin were mock-infected or infected with Sendai virus (SeV). Right: HEK293T cells transfected with HA-ubiquitin were treated (or not) with IFN- β and/or infected, as indicated, with Sendai virus before

immunoprecipitation with anti-RIG-I antibody. **d**, The red lysine residues indicate the sites of ubiquitination. Bottom-left panel: Coomassie-blue-stained Flag-RIG-I(2CARD) complex. NS, nonspecific protein. Bottom-right panel: Lys 29/48/63-linked ubiquitination of RIG-I(2CARD)²¹. **e**, GST pull down (PD) of HEK293T cells transfected with GST-RIG-I(2CARD) or K \rightarrow R mutants. Arrows indicate the ubiquitinated bands. WT, wild type. **f**, IFN- β and NF- κ B promoter activity in GST-RIG-I(2CARD) or K \rightarrow R mutant transfected cells. The results are expressed as means \pm s.d. ($n = 3$).

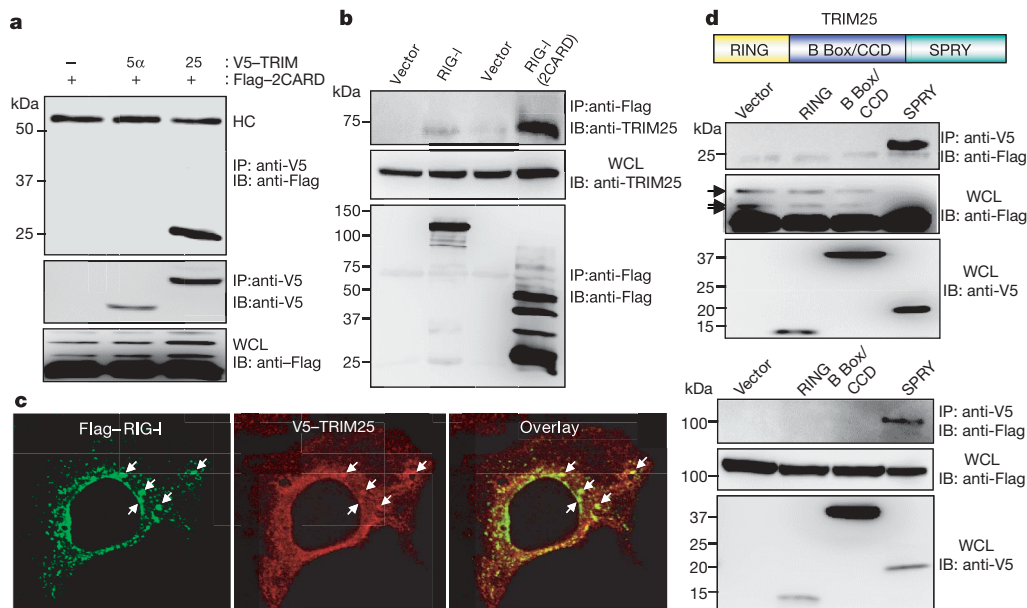


Figure 2 | Interaction between RIG-I and TRIM25. **a**, **b**, WCLs of HEK293T cells transfected with Flag-RIG-I(2CARD) and V5-TRIM25 or V5-TRIM25- α (**a**), or with Flag-RIG-I or Flag-RIG-I(2CARD) (**b**) were used for immunoprecipitation and immunoblotting, as indicated. **c**, Confocal images of HeLa cells transiently transfected with Flag-RIG-I (green) and V5-TRIM25 (red). Arrows indicate representative co-localization between

Flag-RIG-I and V5-TRIM25. Original magnification, $\times 100$. **d**, WCLs of HEK293T cells transfected with Flag-tagged RIG-I(2CARD) (top) or full-length Flag-RIG-I (bottom) together with V5-tagged domains of TRIM25 were used for immunoprecipitation with V5 antibody, followed by immunoblotting with anti-Flag. WCLs were used for immunoblotting with anti-Flag and anti-V5 antibodies.

and that the extent of RIG-I 2CARD ubiquitination correlates strongly with its signal transduction activity.

Protein purification and mass spectrometry demonstrated that TRIM25 (also called oestrogen-responsive finger protein (EFP)¹¹) is one of the proteins that associates with Flag-RIG-I(2CARD). TRIM25 has ubiquitin and ISG15 E3 ligase activity and downregulates 14-3-3 σ through proteolysis for cell cycle regulation^{12,13}. Co-immunoprecipitation revealed that RIG-I(2CARD) interacts with TRIM25 but not TRIM5- α , which has a similar structure to TRIM25 and functions as an intracellular inhibitor of retroviral replication⁷ (Fig. 2a). Furthermore, interaction between Flag-tagged RIG-I or RIG-I(2CARD) and endogenous TRIM25 was readily detected in HEK293T cells (Fig. 2b). Confocal microscopy revealed that both RIG-I and TRIM25 exhibited punctate staining throughout the cytoplasm and that they co-localized extensively at cytoplasmic perinuclear bodies (Fig. 2c). As with other TRIM family members⁷, TRIM25 contains a cluster of a RING-finger domain, a B box/coiled-coil domain (B Box/CCD) and a SPRY domain (Fig. 2d). Binding analysis revealed that the C-terminal SPRY domain of TRIM25 bound to both RIG-I and RIG-I(2CARD) as effectively as full-length TRIM25, whereas the RING-finger domain and B Box/CCD did not (Fig. 2d).

To test the role of TRIM25 in RIG-I ubiquitination, RIG-I or GST-RIG-I(2CARD) was co-expressed with wild-type TRIM25, E3 ligase-defective TRIM25(Δ RING) or TRIM5- α . TRIM25 expression markedly increased the ubiquitination levels of exogenous RIG-I and GST-RIG-I(2CARD), as well as endogenous RIG-I, but neither TRIM25(Δ RING) nor TRIM5- α had any effect (Fig. 3a, b; see also Supplementary Fig. 4a). In contrast, TRIM25 expression did not induce the ubiquitination of GST-MDA5(2CARD) (Supplementary Fig. 4b). TRIM25 depletion *in vivo* by a TRIM25-specific small hairpin RNA (shRNA)¹³ significantly reduced the ubiquitination level of GST-RIG-I(2CARD) and RIG-I in a dose-dependent manner (Fig. 3c and Supplementary Fig. 5a), but a nonspecific scrambled-sequence shRNA had no effect on GST-RIG-I(2CARD) ubiquitination (Supplementary Fig. 5b). Finally, an *in vitro* ubiquitination assay showed that TRIM25 effectively delivered the ubiquitin moieties to maltose-binding protein (MBP)-T7-tagged RIG-I(2CARD), but not MBP-T7 alone or MBP-T7-RIG-I(2CARD(170stop)) (Fig. 3d and Supplementary Fig. 6a). Consistent with its ubiquitination level, RIG-I-mediated induction of IFN- β or NF- κ B promoter activity considerably increased on TRIM25 expression in a dose-dependent manner (Fig. 3e and Supplementary Fig. 6b). Notably, expression of the TRIM25(SPRY) mutant, which was sufficient to bind to RIG-I, markedly suppressed GST-RIG-I(2CARD) ubiquitination in a dose-dependent manner (Fig. 3f) as well as endogenous RIG-I ubiquitination (Supplementary Fig. 4a). Furthermore, expression of the TRIM25(SPRY) mutant considerably decreased the RIG-I 2CARD-mediated activation of IFN- β or NF- κ B promoter activity in a dose-dependent manner (Supplementary Fig. 7). This suggests that TRIM25-mediated ubiquitination has an important role in RIG-I signalling activity.

Unlike the GST-RIG-I(2CARD) K172R mutant, which showed an almost complete loss of ubiquitination and IFN- β and NF- κ B promoter activation, GST-RIG-I(2CARD) K172only—containing five K \rightarrow R substitutions but leaving K172 intact—demonstrated highly induced IFN- β and NF- κ B promoter activity (Fig. 4a, b). Furthermore, the GST-RIG-I(2CARD) K172only mutant underwent robust ubiquitination (albeit lower than that of wild-type GST-RIG-I(2CARD)) on TRIM25 expression, whereas GST-RIG-I(2CARD) K172R was minimally ubiquitinated (Fig. 4c). However, despite a significant reduction in its level of ubiquitination, GST-RIG-I(2CARD) K172R interacted with TRIM25 as efficiently as wild-type GST-RIG-I(2CARD) and the K172only mutant (Fig. 4c). As seen with RIG-I(2CARD), full-length RIG-I K172only but not RIG-I K172R demonstrated ubiquitination at the same level as RIG-I wild type (Supplementary Fig. 8). Finally, correlated with their ubiquitination levels, expression of wild-type RIG-I and mutant RIG-I K172only in

RIG-I^{-/-} mouse embryonic fibroblasts (MEFs) induced IFN- β production on Sendai virus infection, whereas expression of mutant RIG-I K172R showed no effect on IFN- β production (Supplementary Fig. 9).

The 2CARD of RIG-I has been shown to bind to the MAVS CARD to elicit downstream signal transduction¹⁴⁻¹⁷. GST pull-down analysis showed that wild-type GST-RIG-I(2CARD) and mutant GST-RIG-I(2CARD) K172only efficiently interacted with the Flag-tagged CARD proline-rich domain of MAVS (Flag-MAVS(CARD-PRD)), whereas GST-RIG-I(2CARD) K172R and GST-RIG-I(2CARD) K99,169,172,181,190,193R mutants poorly bound to Flag-MAVS(CARD-PRD) (Fig. 4d), indicating that Lys 172 is critical for TRIM25-mediated ubiquitination, RIG-I signalling and MAVS interaction, but not for TRIM25 binding (Fig. 4c).

Wild-type, *Trim25*^{+/-} and *Trim25*^{-/-} MEFs¹⁸ were used to test the direct contribution of TRIM25 to RIG-I-mediated IFN- β expression. IFN- β promoter activity was very low in *Trim25*^{-/-} MEFs and was reduced in *Trim25*^{+/-} MEFs compared with wild-type MEFs

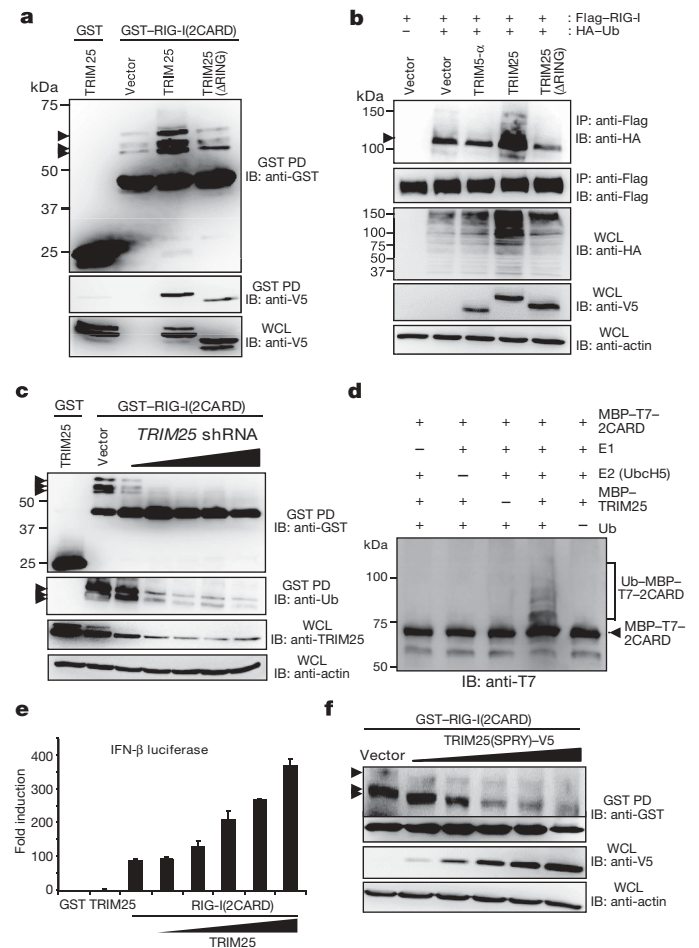


Figure 3 | TRIM25 is a primary E3 ubiquitin ligase of RIG-I. HEK293T cells transfected with GST or GST-RIG-I(2CARD) (**a**) or Flag-RIG-I and HA-ubiquitin (**b**) together with vector, TRIM25, TRIM25(Δ RING) or TRIM5- α were used for GST pull down (PD) (**a**) or immunoprecipitation with anti-Flag antibody (**b**). **c**, HEK293T cells transfected with GST or GST-RIG-I(2CARD) together with pSUPER.retro.puro or TRIM25-shRNA-specific pSUPER.retro.puro¹³ were used for GST pull down. Arrows indicate the ubiquitinated GST-RIG-I(2CARD) and Flag-RIG-I. **d**, *In vitro* ubiquitination was detected by anti-T7 immunoblotting. **e**, IFN- β luciferase activity in HEK293T cells transfected with GST-RIG-I(2CARD) and TRIM25. The results are expressed as means \pm s.d. (n = 3). **f**, HEK293T cells transfected with GST-RIG-I(2CARD) and V5-TRIM25(SPRY) were used for GST pull down. Arrows indicate ubiquitinated GST-RIG-I(2CARD).

(Supplementary Fig. 10a). Consistent with IFN- β promoter activation, virus-induced IFN- β production was virtually undetectable in *Trim25*^{-/-} MEFs, whereas it was considerably high in wild-type MEFs (Fig. 4e). *Trim25*^{+/-} MEFs showed a slightly reduced level of IFN- β production compared with wild-type MEFs (Fig. 4e). On vesicular stomatitis virus (VSV)-enhanced green fluorescent protein (eGFP) infection at various multiplicity of infections (MOIs), *Trim25*^{-/-} MEFs showed remarkably increased levels of VSV-eGFP-positive cells (Fig. 4g and Supplementary Fig. 10b) and increased VSV yields (over 100-fold) (Fig. 4f) compared with wild-type and *Trim25*^{+/-} MEFs. Similarly, *Trim25*^{-/-} MEFs showed a considerable increase in the level of Newcastle disease virus (NDV)-GFP infection (Supplementary Fig. 10c). Finally, TRIM25 expression significantly suppressed VSV-eGFP replication in HEK293T cells, whereas expression of the TRIM25(SPRY) mutant detectably increased VSV-eGFP replication (Fig. 4h). Collectively, these results indicate that TRIM25 is critical for cytosolic RIG-I signal transduction that mediates the induction of the IFN response on viral infection.

Ubiquitination is a versatile post-translational modification involved in various cellular functions¹⁹. Our study indicates that

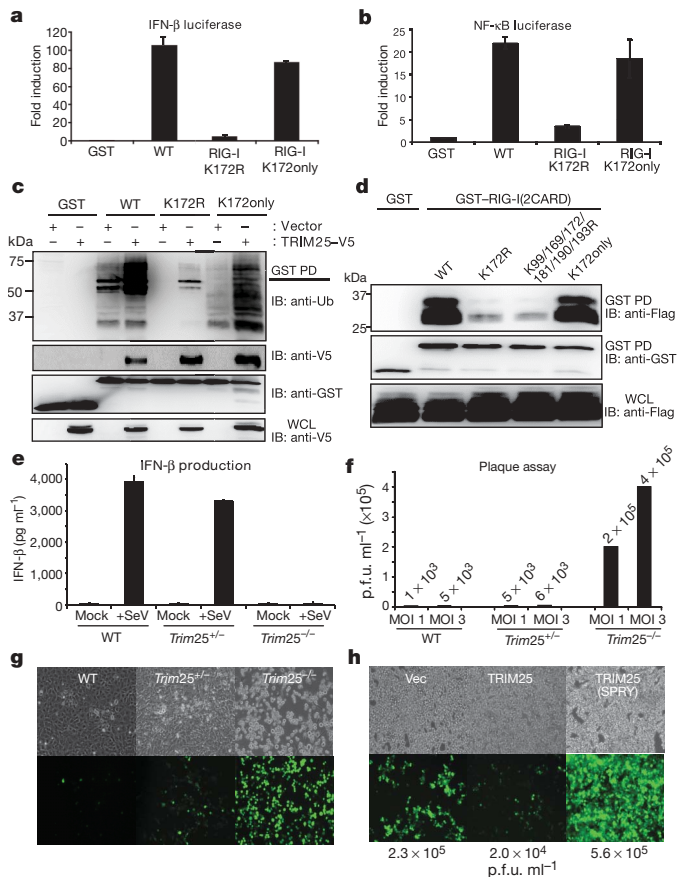


Figure 4 | Role of TRIM25-mediated ubiquitination in RIG-I antiviral activity. IFN- β (a) and NF- κ B (b) promoter activity in GST-RIG-I(2CARD) or mutant transfected cells. The results are expressed as means \pm s.d. ($n = 3$). c, HEK293T cells transfected with GST-RIG-I(2CARD), GST-RIG-I(2CARD) K172R, or GST-RIG-I(2CARD) K172only together with vector or TRIM25 were used for GST pull down. d, HEK293T cells transfected with GST-RIG-I(2CARD) or the indicated mutants together with Flag-MAVS(CARD-PRD) were used for GST pull down. e, IFN- β production in wild-type, *Trim25*^{+/-} and *Trim25*^{-/-} MEFs upon Sendai virus infection. The results are expressed as means \pm s.d. ($n = 3$). f-h, VSV-eGFP replication in wild-type, *Trim25*^{+/-} and *Trim25*^{-/-} MEFs (f and g) or in vector-, TRIM25-, or TRIM25(SPRY)-expressing HEK293T cells (h) was determined by plaque assay or visualized by fluorescence microscopy.

TRIM25 E3 ubiquitin ligase induces the Lys 63-linked ubiquitination of RIG-I; that Lys 172 is the critical site for TRIM25-mediated ubiquitination; and that, as seen with the ubiquitin-dependent interaction between RIP and NEMO²⁰, the TRIM25-mediated ubiquitination of RIG-I may facilitate its interaction with MAVS, which ultimately leads to downstream signal transduction. Thus, the interconnection between the RIG-I cytosolic viral RNA receptor and a member of the TRIM family represents a new class of antiviral regulatory pathway involved in innate immunity.

METHODS SUMMARY

RNA interference for TRIM25. The mammalian expression vector pSUPER-retro.puro (OligoEngine), encoding shRNAs for *TRIM25* sequence, was provided by D.-E. Zhang. Details of the shRNA sequence and transfection method have been described¹³.

Viruses. NDV-GFP and VSV-eGFP were provided by A. Garcia-Sastre and S. Whelan, respectively.

Measurement of IFN- β production. Cell culture supernatants were collected and analysed for IFN- β production using enzyme-linked immunosorbent assays (PBL Biomedical Laboratories).

In vitro ubiquitination assay. Purified MBP-T7-RIG-I(2CARD) (20 μ g ml⁻¹) and MBP-TRIM25 (20 μ g ml⁻¹) derived from *Escherichia coli* were incubated in a reaction buffer (50 mM Tris-HCl, 2 mM dithiothreitol, 5 mM MgCl₂ and 4 mM ATP) with ubiquitin (50 μ g ml⁻¹; Sigma), human recombinant E1 (1.6 μ g ml⁻¹; BIOMOL) and human recombinant UbcH5a (20 μ g ml⁻¹; BIOMOL) at 32 °C for 2 h and subjected to immunoblotting with anti-T7 antibody (Novagen).

Full Methods and any associated references are available in the online version of the paper at www.nature.com/nature.

Received 14 February; accepted 8 March 2007.

Published online 28 March 2007.

- Honda, K., Takaoka, A. & Taniguchi, T. Type I interferon gene induction by the interferon regulatory factor family of transcription factors. *Immunity* 25, 349–360 (2006); erratum 25, 849 (2006).
- Hornung, V. et al. 5'-Triphosphate RNA is the ligand for RIG-I. *Science* 314, 994–997 (2006).
- Meylan, E. & Tschopp, J. Toll-like receptors and RNA helicases: two parallel ways to trigger antiviral responses. *Mol. Cell* 22, 561–569 (2006).
- Pichlmair, A. et al. RIG-I-mediated antiviral responses to single-stranded RNA bearing 5'-phosphates. *Science* 314, 997–1001 (2006).
- Stetson, D. B. & Medzhitov, R. Antiviral defense: interferons and beyond. *J. Exp. Med.* 203, 1837–1841 (2006).
- Yoneyama, M. et al. The RNA helicase RIG-I has an essential function in double-stranded RNA-induced innate antiviral responses. *Nature Immunol.* 5, 730–737 (2004).
- Nisole, S., Stoye, J. P. & Saib, A. TRIM family proteins: retroviral restriction and antiviral defence. *Nature Rev. Microbiol.* 3, 799–808 (2005).
- Johnson, C. L. & Gale, M. Jr. CARD games between virus and host get a new player. *Trends Immunol.* 27, 1–4 (2006).
- Meylan, E., Tschopp, J. & Karin, M. Intracellular pattern recognition receptors in the host response. *Nature* 442, 39–44 (2006).
- Kato, H. et al. Cell type-specific involvement of RIG-I in antiviral response. *Immunity* 23, 19–28 (2005).
- Orimo, A., Inoue, S., Ikeda, K., Noji, S. & Muramatsu, M. Molecular cloning, structure, and expression of mouse estrogen-responsive finger protein Efp. Co-localization with estrogen receptor mRNA in target organs. *J. Biol. Chem.* 270, 24406–24413 (1995).
- Urano, T. et al. Efp targets 14-3-3 σ for proteolysis and promotes breast tumour growth. *Nature* 417, 871–875 (2002).
- Zou, W. & Zhang, D. E. The interferon-inducible ubiquitin-protein isopeptide ligase (E3) EFP also functions as an ISG15 E3 ligase. *J. Biol. Chem.* 281, 3989–3994 (2006).
- Meylan, E. et al. Cardif is an adaptor protein in the RIG-I antiviral pathway and is targeted by hepatitis C virus. *Nature* 437, 1167–1172 (2005).
- Seth, R. B., Sun, L., Ea, C. K. & Chen, Z. J. Identification and characterization of MAVS, a mitochondrial antiviral signaling protein that activates NF- κ B and IRF 3. *Cell* 122, 669–682 (2005).
- Xu, L. G. et al. VISA is an adaptor protein required for virus-triggered IFN- β signaling. *Mol. Cell* 19, 727–740 (2005).
- Kawai, T. et al. IPS-1, an adaptor triggering RIG-I- and Mda5-mediated type I interferon induction. *Nature Immunol.* 6, 981–988 (2005).
- Orimo, A. et al. Underdeveloped uterus and reduced estrogen responsiveness in mice with disruption of the estrogen-responsive finger protein gene, which is a direct target of estrogen receptor α . *Proc. Natl Acad. Sci. USA* 96, 12027–12032 (1999).

19. Haglund, K. & Dikic, I. Ubiquitylation and cell signaling. *EMBO J.* **24**, 3353–3359 (2005).
20. Ea, C. K., Deng, L., Xia, Z. P., Pineda, G. & Chen, Z. J. Activation of IKK by TNF α requires site-specific ubiquitination of RIP1 and polyubiquitin binding by NEMO. *Mol. Cell* **22**, 245–257 (2006).
21. Kirkpatrick, D. S., Denison, C. & Gygi, S. P. Weighing in on ubiquitin: the expanding role of mass-spectrometry-based proteomics. *Nature Cell Biol.* **7**, 750–757 (2005).

Supplementary Information is linked to the online version of the paper at www.nature.com/nature.

Acknowledgements This work was supported by US Public Health Service grants (J.U.J.), the exchange programme between Harvard Medical School and the graduate training programme 1071 at the Friedrich-Alexander University Erlangen-Nuremberg, Germany (M.U.G.), and a Korea Research Foundation Grant (C.-H.J.). We thank A. Garcia-Sastre, D.-E. Zhang and S. Whelan for providing

reagents, and R. Tomaino and J. Nagel for mass spectrometry. We also thank all members of the Tumor Virology Division, New England Primate Research Center, for discussions.

Author Contributions M.U.G. performed all aspects of this study. Y.C.S., C.-H.J. and C.L. assisted in experimental design and in collecting the data. T.U. and S.I. performed the *in vitro* ubiquitination assay and generated *Trim25*^{-/-} MEFs. L.S. and Z.C. generated the MAVS construct and RIG-I antibody. T.O. and S.A. generated the RIG-I construct and *RIG-I*^{-/-} MEFs. M.U.G. and J.U.J. organized this study and wrote the paper. All authors discussed the results and commented on the manuscript.

Author Information Reprints and permissions information is available at www.nature.com/reprints. The authors declare no competing financial interests. Correspondence and requests for materials should be addressed to J.U.J. (jae_jung@hms.harvard.edu).

METHODS

Cell culture. HEK293T, MEF and HeLa cells were cultured in Dulbecco's modified Eagle's medium supplemented with 10% fetal bovine serum, 2 mM L-glutamine and 1% penicillin-streptomycin (Gibco-BRL). Transient transfections were performed with FuGENE 6 (Roche), lipofectamine 2000 (Invitrogen), or calcium phosphate (Clontech) following the manufacturer's instructions. Wild-type, *Trim25*^{+/-} and *Trim25*^{-/-} MEFs were immortalized with LXSNE6/E7 retroviral vector containing human papilloma virus 16 E6 and E7 oncogenes using a standard protocol of selection with 200 µg ml⁻¹ of neomycin. *RIG-I*^{-/-} MEFs were infected with pBabe-puro vector, pBabe-puro-RIG-I wild-type, pBabe-puro-RIG-I K172R, or pBabe-puro-RIG-I K172only retrovirus, followed by selection with 1 µg ml⁻¹ of puromycin.

Plasmid construction. All constructs for transient and stable expression in mammalian cells were derived from the pEBG GST fusion vector and the pEF-IRES-Puro expression vector. DNA fragments corresponding to the coding sequence of the *RIG-I* and *TRIM25* genes were amplified from template DNA by polymerase chain reaction (PCR) and subcloned into plasmid pEBG between restriction sites *KpnI* and *NotI* or pEF-IRES-puro between *AflIII* and *NotI* for selection of stable transfectants. V5-tagged TRIM25 and Flag-tagged RIG-I were expressed from a modified pIRES-puro encoding a C-terminal V5 tag and Flag tag, respectively. RIG-I mutants were generated by PCR using site-directed mutagenesis. All constructs were sequenced using an ABI PRISM 377 automatic DNA sequencer to verify 100% agreement with the original sequence.

In vivo GST pull down, protein purification and mass spectrometry. At 48 h after transfection with vectors expressing GST, GST-RIG-I(2CARD) or GST-MDA5(2CARD) fusions, HEK293T cells were collected and lysed with NP40 buffer (50 mM HEPES, pH 7.4, 150 mM NaCl, 1 mM EDTA, 1% (v/v) NP40) supplemented with a complete protease inhibitor cocktail (Roche). Post-centrifuged supernatants were pre-cleared with protein A/G beads at 4 °C for 2 h. Pre-cleared lysates were mixed with a 50% slurry of glutathione-conjugated Sepharose beads (Amersham Biosciences), and the binding reaction was incubated for 4 h at 4 °C. Precipitates were washed extensively with lysis buffer. Proteins bound to glutathione beads were eluted and separated on a NuPAGE 4–12% Bis-Tris gradient gel (Invitrogen). After Coomassie or silver staining (Invitrogen), specific protein bands were excised and analysed by ion-trap mass spectrometry at the Harvard Taplin Biological Mass Spectrometry facility, and amino acid sequences were determined by tandem mass spectrometry and database searches.

Immunoblot analysis and immunoprecipitation assay. For immunoblotting, polypeptides were resolved by SDS-polyacrylamide gel electrophoresis (SDS-PAGE) and transferred to a PVDF membrane (Bio-Rad). Immunodetection was achieved with anti-V5 (1:5,000) (Invitrogen), anti-Flag (1:5,000) (Sigma), anti-HA (1:5,000), anti-GST (1:10,000) (Sigma), anti-actin (1:10,000) (Abcam), or anti-TRIM25 (1:2,000) (BD Bioscience) antibodies. The proteins were visualized by a chemiluminescence reagent (Pierce) and detected by a Fuji Phosphor Imager.

For immunoprecipitation, cells were collected after 48 h and then lysed in NP40 buffer supplemented with a complete protease inhibitor cocktail (Roche). After pre-clearing with protein A/G agarose beads for 2 h at 4 °C, whole-cell lysates were used for immunoprecipitation with the indicated antibodies. Generally, 1–2 µg of commercial antibody was added to 1 ml of cell lysate, which was incubated at 4 °C for 4–12 h. After addition of protein A/G agarose beads, the incubation was continued for 2 h. Immunoprecipitates were extensively washed with lysis buffer and eluted with SDS loading buffer by boiling for 5 min.

Confocal immunofluorescence microscopy. Eighteen to twenty-four hours after transfection, cells were fixed with 4% paraformaldehyde for 15 min, permeabilized with 0.2% (v/v) Triton X-100 for 15 min, blocked with 10% goat serum in PBS for 1 h and reacted with diluted primary antibody in 1% goat serum for up to 2 h at room temperature. After incubation, cells were washed extensively with PBS, incubated with the appropriate secondary antibody diluted in 1% goat serum for 1 h at room temperature, and washed three times with PBS. Confocal microscopy was performed using a Leica TCS SP laser-scanning microscope (Leica Microsystems) fitted with a ×100 Leica objective (PL APO, 1.4NA) and Leica imaging software. Images were collected at 512 × 512-pixel resolution. The stained cells were optically sectioned in the z axis, and the images in the different channels (photo multiplier tubes) were collected simultaneously. The step size in the z axis varied from 0.2 to 0.5 µm to obtain 16 slices per imaged file. The images were transferred to a Macintosh G4 computer (Apple Computer), and Photoshop (Adobe) was used to render the images.